Korean Journal of Radiology

KJR

Check for updates

Intraindividual Comparison of Hepatocellular Carcinoma Washout between MRIs with Hepatobiliary and Extracellular Contrast Agents

Yeun-Yoon Kim[1]*, Young Kon Kim[1], Ji Hye Min[1], Dong Ik Cha[1], Jong Man Kim[2], Gyu-Seong Choi[2], Soohyun Ahn[3]

Departments of [1]Radiology and Center for Imaging Science and [2]Surgery, Samsung Medical Center, Sungkyunkwan University School of Medicine, Seoul, Korea; [3]Department of Mathematics, Ajou University, Suwon, Korea

Objective: To intraindividually compare hepatocellular carcinoma (HCC) washout between MRIs using hepatobiliary agent (HBA) and extracellular agent (ECA).

Materials and Methods: This study included 114 prospectively enrolled patients with chronic liver disease (mean age, 55 ± 9 years; 94 men) who underwent both HBA-MRI and ECA-MRI before surgical resection for HCC between November 2016 and May 2019. For 114 HCCs, the lesion-to-liver visual signal intensity ratio (SIR) using a 5-point scale (-2 to +2) was evaluated in each phase. Washout was defined as negative visual SIR with temporal reduction of visual SIR from the arterial phase. Illusional washout (IW) was defined as a visual SIR of 0 with an enhancing capsule. The frequency of washout and MRI sensitivity for HCC using LR-5 or its modifications were compared between HBA-MRI and ECA-MRI. Subgroup analysis was performed according to lesion size (< 20 mm or ≥ 20 mm).

Results: The frequency of portal venous phase (PP) washout with HBA-MRI was comparable to that of delayed phase (DP) washout with ECA-MRI (77.2% [88/114] vs. 68.4% [78/114]; p = 0.134). The frequencies were also comparable when IW was allowed (79.8% [91/114] for HBA-MRI vs. 81.6% [93/114] for ECA-MRI; p = 0.845). The sensitivities for HCC of LR-5 (using PP or DP washout) were comparable between HBA-MRI and ECA-MRI (78.1% [89/114] vs. 73.7% [84/114]; p = 0.458). In HCCs < 20 mm, the sensitivity of LR-5 was higher on HBA-MRI than on ECA-MRI (70.8% [34/48] vs. 50.0% [24/48]; p = 0.034). The sensitivity was similar to each other if IW was added to LR-5 (72.9% [35/48] for HBA-MRI vs. 70.8% [34/48] for ECA-MRI; p > 0.999).

Conclusion: Extracellular phase washout for HCC diagnosis was comparable between MRIs with both contrast agents, except for tumors < 20 mm. Adding IW could improve the sensitivity for HCC on ECA-MRI in tumors < 20 mm.

Keywords: *Gadoxetic acid; Extracellular contrast; Magnetic resonance imaging; Hepatocellular carcinoma; Washout*

INTRODUCTION

Washout is an essential imaging feature for the noninvasive diagnosis of hepatocellular carcinoma (HCC) [1]. Liver Imaging Reporting and Data System (LI-RADS) is a comprehensive system for the standardized interpretation of liver MRI. LI-RADS defines washout as "non-peripheral visually assessed temporal reduction in enhancement relative to composite liver tissue from earlier to later phase resulting in hypoenhancement in the extracellular phase" in which liver parenchymal enhancement is mainly attributable to the extracellular distribution of contrast [2]. The term

"non-peripheral" is considered a better definition to exclude non-HCC malignancies and enable a more specific diagnosis for HCC [3]. Additionally, the "visual" assessment of washout is practical since quantitative criteria for washout have not been established [4,5]. However, the concept of temporal reduction in enhancement has not yet been validated; many researchers still use hypoenhancement in the extracellular phase as washout. In this regard, the semi-quantitative analysis of signal intensity on each dynamic phase may help determine the presence of temporal reduction in enhancement.

The LI-RADS definition of washout excludes an optical illusion of washout in the presence of an enhancing capsule, which has been described on the extracellular agent (ECA)-enhanced MRI (ECA-MRI) (i.e., illusional washout [IW]) [2]. However, it may be difficult to strictly differentiate IW from true washout by visual assessment [4], which can result in variability of the decision between LI-RADS categories 4 and 5 for lesions sized 10–19 mm [6]. Interestingly, incorporating IW into the washout definition may improve the sensitivity for HCC without compromising the specificity [7].

Gadoxetic acid, a hepatobiliary agent (HBA), is actively taken up by functioning hepatocytes, and approximately half of the injected dose is excreted into the biliary system [8]. As liver parenchymal enhancement is apparent in the transitional phase (TP), which is acquired 2–5 minutes after gadoxetic acid injection, TP hypointensity can represent either true de-enhancement of HCC or a pseudo-washout of non-HCC lesions [9,10]. Therefore, evaluation of washout is currently not allowed in TP [2,11]. This could be problematic as washout perceivable only in the delayed phase (DP) of ECA-MRI, the counterpart of TP, may not be considered on HBA-MRI, especially in HCCs showing persistent enhancement in portal venous phase (PP) [12,13]. Meanwhile, as hepatocyte uptake of gadoxetic acid begins at approximately 60–90 seconds after contrast injection [13,14], washout in the PP of gadoxetic acid-enhanced MRI (HBA-MRI) might be more conspicuous than that of ECA-MRI. Therefore, applying extracellular phase washout on HBA-MRI may have both advantages and disadvantages when compared to that on ECA-MRI. While extracellular phase washout in LI-RADS refers to PP washout with HBA-MRI and PP or DP washout with ECA-MRI, comparing the frequency of extracellular phase washout on both MRIs may offer important insights into understanding the different pharmacokinetics of MRI contrast agents.

To the best of our knowledge, there is no published study that focuses on the comparison of washout between HBA-MRI and ECA-MRI in an intraindividual manner. Therefore, we devised this study to intraindividually compare HCC washout between HBA-MRI and ECA-MRI.

MATERIALS AND METHODS

Patients

The Institutional Review Board of Samsung Medical Center approved this study (registration number: 2019-12-105), which involved a retrospective review of medical records and images in a prospectively recruited patient cohort. Under a prospective study protocol, written informed consent was obtained from 136 patients with chronic liver disease for the preoperative evaluation of hepatic tumors using MRIs with gadoxetic acid (HBA-MRI) and gadoterate meglumine (ECA-MRI) from November 2016 to May 2019. Inclusion criteria were (a) treatment-naïve patients with chronic liver disease or liver cirrhosis and (b) histopathologic diagnosis of HCC from the surgical specimen. The exclusion criterion was HCC with a targetoid appearance showing either rim arterial phase hyperenhancement (APHE) or peripheral washout [6], which was assessed in a preliminary image analysis session by a study coordinator (with 10 years of experience in liver imaging). If a patient had more than one HCC, the largest HCC was selected for analysis by the coordinator. Therefore, 114 patients with 114 non-targetoid HCCs were included in the analysis. Fifty-eight (50.9%) of the 114 patients had been included in a previous study [7], which reported on the comparison of the diagnostic performance between HBA-MRI and ECA-MRI. This study focused on the comparison of non-peripheral washout, which is a major feature for the diagnosis of HCC using LI-RADS v2018 category 5 (LR-5) criteria.

Image Acquisition

MRIs were acquired using a 3T system: Achieva or Ingenia (Philips Healthcare) or Magnetom Skyra (Siemens Healthcare). For dynamic contrast-enhanced imaging, T1-weighted three-dimensional (3D) gradient-echo images were obtained before and after intravenous administration of gadoxetic acid (Primovist, Bayer Healthcare) at an injection rate of 1 mL/s for a total dose of 0.025 mmoL/kg body weight, or gadoterate meglumine (Dotarem, Guerbet) at an injection rate of 2 mL/s for a total dose of 0.1 mmoL/kg body weight. The arterial phase (AP), PP, DP (TP for gadoxetic acid), and hepatobiliary phase (for gadoxetic acid only) images

were obtained at 8 seconds after contrast arrival at the distal thoracic aorta, and at 60 seconds, 3 minutes, and 20 minutes after contrast injection, respectively. The timing of AP was determined using a magnetic resonance fluoroscopic bolus detection technique.

Image Analysis

Two board-certified radiologists (with 6 and 11 years of experience in liver imaging, respectively) independently evaluated the MRIs. The two sets of imaging data were presented to the readers in a side-by-side manner (set A: AP, PP, and TP of HBA-MRI, and set B: AP, PP, and DP of ECA-MRI). The readers were aware that the patients were histopathologically diagnosed with HCC; however, were blinded to the clinical information. Lesion-to-liver visual signal intensity ratio (SIR) was defined as the signal intensity of the lesion relative to the adjacent liver parenchyma as follows [15]: -2, marked hypointensity; -1, mild hypointensity; 0, isointensity; +1, mild hyperintensity; and +2, marked hyperintensity. Any discrepancies in visual SIR between the readers were resolved by consensus reading. The consensus results were used for data analysis.

According to the LI-RADS definition [16], non-rim APHE was defined as a positive visual SIR in the AP. For the analysis of washout, the temporal reduction in enhancement was calculated by subtracting the visual SIR of the latter phases from that of the AP. Washout was defined as negative visual SIR in the latter phase with temporal reduction of visual SIR compared to the AP. The presence of an enhancing capsule in each tumor was also evaluated, and IW was defined as a visual SIR of 0 in the presence of an enhancing capsule [4].

Based on the lesion size and presence or absence of APHE, washout, and enhancing capsule, each lesion was evaluated if it met the LR-5 criteria [6]. Modified LR-5 criteria were defined as LR-5 criteria allowing TP washout on HBA-MRI, or IW on both MRIs as washout. The MRI sensitivities of the LR-5 criteria and modified LR-5 criteria for HCC diagnosis were calculated and compared between HBA-MRI and ECA-MRI. Subgroup analysis was performed according to lesion size (< 20 mm or ≥ 20 mm).

Statistical Analysis

Patient characteristics were summarized descriptively. Visual SIR was compared between HBA-MRI and ECA-MRI using the Wilcoxon signed-rank test, and inter-reader agreement for visual SIR was calculated using

Cohen's weighted κ statistics. The frequency of enhancing capsule was compared using McNemar's test, and inter-reader agreement for enhancing capsule was calculated using Cohen's unweighted κ statistics. κ statistics were interpreted as follows: κ ≤ 0.00, poor agreement; κ = 0.01–0.20, slight agreement; κ = 0.21–0.40, fair agreement; κ = 0.41–0.60, moderate agreement; κ = 0.61–0.80, substantial agreement; and κ = 0.81–0.99, almost perfect agreement. The frequency of washout and MRI sensitivity for HCC using LR-5 or its modifications were compared using McNemar's test. Analyses were performed using R version 3.4.3 (The R Foundation for Statistical Computing). A two-sided p value < 0.05 was considered to be of statistical significance.

RESULTS

Patients Demographics

Of the 136 potentially eligible patients, three patients had a history of HCC, and 15 patients received histopathologic diagnoses of non-HCC lesions. Of the remaining 118 patients, four patients with HCC showing a targetoid appearance were excluded, and 114 patients (94 men and 20 women) were finally included in the study (Fig. 1). The patients had a mean age of 55 ± 9 years (Table 1). Hepatitis B virus infection was present in 99 (86.8%) patients, and liver cirrhosis was present in 71 (62.3%) patients. The majority (n = 106, 93.0%) of patients had Child-Pugh class A liver function. The median time interval between HBA-MRI and ECA-MRI was 20 days (interquartile
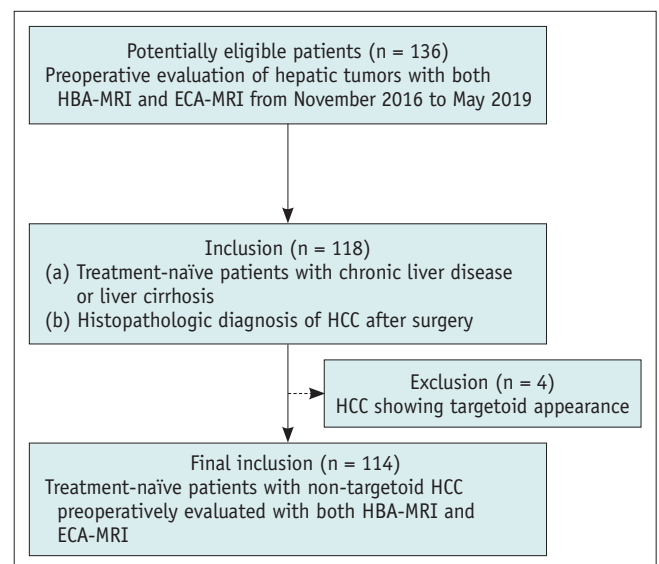
Fig. 1. Flowchart of study participants. ECA = extracellular agent, HBA = hepatobiliary agent, HCC = hepatocellular carcinoma

range [IQR], 16, 25), and the median time interval between HBA-MRI and surgery was 21 days (IQR, 17, 26). The median size of HCC lesions was 22 mm (IQR, 16, 27).

Table 1. Patient Demographics

Variable	Value (n = 114)
Age (year), mean ± SD	55 ± 9
Men/women	94/20
Etiology	
HBV	98 (86.0)
HCV	8 (7.0)
Alcohol	6 (5.3)
HBV and HCV	1 (0.9)
Other	1 (0.9)
Liver cirrhosis	71 (62.3)
Child-Pugh classification	
A	106 (93.0)
B	8 (7.0)
Serum AFP level (ng/mL), median (IQR)	10.3 (3.3, 104.0)
Time interval between HBA-MRI and ECA-MRI (day), median (IQR)	20 (16, 25)
Time interval between HBA-MRI and surgery (day), median (IQR)	21 (17, 26)
Lesion size (mm), median (IQR)	22 (16, 27)

Data are number of patients with percentages in parentheses unless otherwise described. AFP = alpha-fetoprotein, ECA = extracellular agent, HBA = hepatobiliary agent, HBV = hepatitis B virus, HCV = hepatitis C virus, IQR = interquartile range, SD = standard deviation
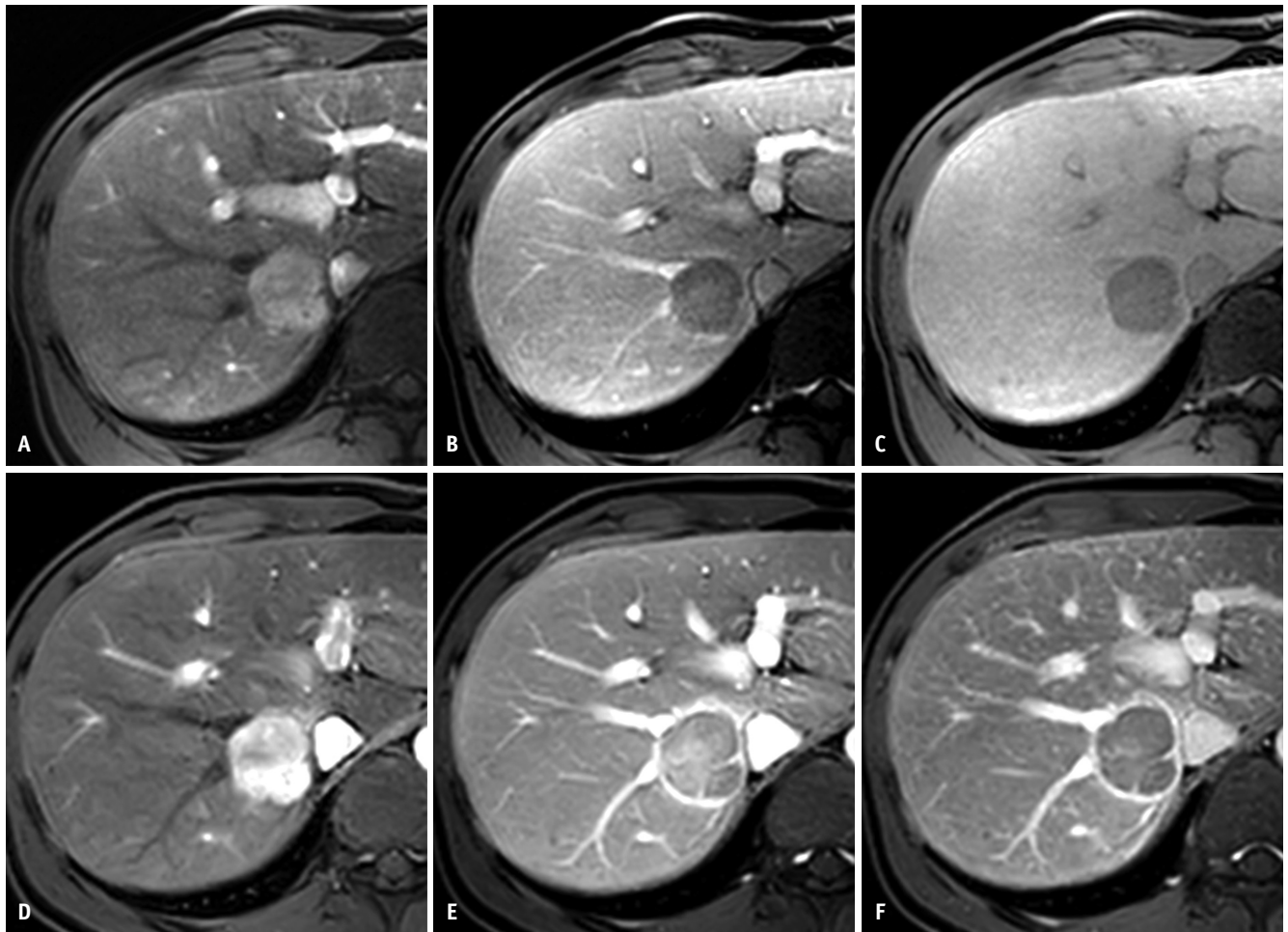
Visual SIR and Enhancing Capsule

Visual SIR in the AP was lower with HBA-MRI than with ECA-MRI ($p = 0.009$) (Table 2); however, the frequency of non-rim APHE (i.e., visual SIR > 0 in AP) was similar between HBA-MRI and ECA-MRI (97.4% [n = 111] vs. 98.2% [n = 112]). Visual SIR in the PP of HBA-MRI was lower than that of ECA-MRI ($p < 0.001$); however, did not differ from that in the DP of ECA-MRI ($p = 0.102$) (Fig. 2). Visual SIR in the TP was even lower than that in the DP ($p < 0.001$). Inter-reader agreement for visual SIR was substantial to almost perfect throughout all phases with HBA-MRI (κ, 0.67–0.95) and ECA-MRI (κ, 0.62–0.84).

An enhancing capsule was less frequently observed with HBA-MRI than with ECA-MRI (37.7% [n = 43] vs. 75.4% [n = 86]; $p < 0.001$). Inter-reader agreement for enhancing capsule was moderate for both HBA-MRI (κ = 0.56) and ECA-MRI (κ = 0.59).

Washout

The frequencies of HCC washout are summarized in Table 3. With HBA-MRI, IW was present in three (11.5%) of 26 lesions without washout in PP, and in two (25.0%) of eight lesions without washout in TP. With ECA-MRI, IW was present in 22 (40.0%) of 55 lesions without washout in PP, and in 15 (41.7%) of 36 lesions without washout in DP (Fig. 3). The PP washout was more frequent on HBA-

Table 2. Results of Visual SIR Analysis (n = 114)

Phase	Visual SIR*				κ (95% CI)	
	Value	HBA	ECA	P	HBA	ECA
AP	-2	1 (0.9)	0 (0)	0.009	0.76 (0.63, 0.89)	0.84 (0.70, 0.98)
	-1	1 (0.9)	0 (0)			
	0	1 (0.9)	2 (1.8)			
	+1[†]	31 (27.2)	17 (14.9)			
	+2[†]	80 (70.2)	95 (83.3)			
PP	-2	60 (52.6)	32 (28.1)	< 0.001	0.68 (0.62, 0.82)	0.73 (0.69, 0.84)
	-1	29 (25.4)	27 (23.7)			
	0	14 (12.3)	19 (16.7)			
	+1	3 (2.6)	10 (8.8)			
	+2	8 (7.0)	26 (22.8)			
TP/DP	-2	91 (79.8)	55 (48.3)	< 0.001	0.67 (0.60, 0.86)	0.62 (0.67, 0.80)
	-1	16 (14.0)	23 (20.2)			
	0	4 (3.5)	17 (14.9)			
	+1	1 (0.9)	8 (7.0)			
	+2	2 (1.8)	11 (9.7)			

Data are number of lesions with percentages in parentheses. *Visual SIR was defined as signal intensity of lesion relative to adjacent liver parenchyma as follows: -2, marked hypointensity; -1, mild hypointensity; 0, isointensity; +1, mild hyperintensity; and +2, marked hyperintensity, [†]Positive visual SIR in the AP indicates the presence of non-rim AP hyperenhancement. AP = arterial phase, CI = confidence interval, DP = delayed phase, ECA = extracellular agent, HBA = hepatobiliary agent, PP = portal venous phase, SIR = signal intensity ratio, TP = transitional phase

Fig. 2. A 46-year-old man with hepatitis B-related liver cirrhosis and hepatocellular carcinoma.
A-C. On the axial T1-weighted 3D turbo field-echo images obtained after gadoxetic acid injection, a 35 mm mass at hepatic segment VII shows **(A)** non-rim APHE (lesion-to-liver visual SIR, +2), **(B)** PP washout (visual SIR, -2; temporal reduction in enhancement from AP, -4), and **(C)** transitional phase washout (visual SIR, -2). **D-F.** On the axial T1-weighted 3D turbo field-echo images obtained after gadoterate meglumine administration, the mass reveals **(D)** non-rim APHE (visual SIR, +2), **(E)** mild hyperintensity (visual SIR, +1) and an enhancing capsule in PP, and **(F)** delayed phase washout (visual SIR, -2; temporal reduction in enhancement from AP, -4). LR-5 category was assigned on both MRIs by both readers using extracellular phase washout. AP = arterial phase, APHE = arterial phase hyperenhancement, LR-5 = Liver Imaging Reporting and Data System category 5, PP = portal venous phase, SIR = signal intensity ratio, 3D = three-dimensional

MRI than ECA-MRI (77.2% vs. 51.8%; $p < 0.001$); however, was comparable when IW was allowed (79.8% for HBA-MRI vs. 71.1% for ECA-MRI; $p = 0.078$). The frequency of PP washout with HBA-MRI was comparable to that of DP washout with ECA-MRI (77.2% vs. 68.4%; $p = 0.134$); the frequencies were also comparable when IW was allowed (79.8% for HBA-MRI vs. 81.6% for ECA-MRI; $p = 0.845$) (Fig. 4). TP washout was more frequent than DP washout (93.0% vs. 68.4%; $p < 0.001$); however, the difference was smaller when IW was allowed (94.7% for HBA-MRI vs. 81.6% for ECA-MRI; $p = 0.004$).

Sensitivity for HCC
The sensitivity of LR-5 criteria using PP washout with HBA-MRI was comparable to that using DP washout with ECA-MRI (78.1% vs. 73.7%; $p = 0.458$); the sensitivities were also comparable when IW was allowed (79.0% for HBA-MRI vs. 82.5% for ECA-MRI; $p = 0.540$) (Table 4, Fig. 5). Allowing IW enabled the diagnosis of one more HCC on HBA-MRI and 10 more HCCs on ECA-MRI, which were all less than 20 mm in size. In tumors smaller than 20 mm, the sensitivity of LR-5 criteria using PP washout with HBA-MRI was higher than that using DP washout with ECA-MRI (70.8% vs. 50.0%; $p = 0.034$); however, was nearly identical to that using DP washout with ECA-MRI when IW was also allowed (72.9% for HBA-MRI vs. 70.8% for ECA-MRI; $p > 0.999$). In tumors larger than 20 mm, the sensitivity of HBA-MRI did not show a significant difference from that of ECA-MRI

Table 3. Comparison of Washout according to MRI Contrast Media (n = 114)

Phase (HBA/ECA)	Washout	HBA	ECA	P
Presence or absence of washout				
PP/PP	Yes	88 (77.2)	59 (51.8)	< 0.001
	No	26 (22.8)	55 (48.2)	
PP/DP	Yes	88 (77.2)	78 (68.4)	0.134
	No	26 (22.8)	36 (31.6)	
TP/DP	Yes	106 (93.0)	78 (68.4)	< 0.001
	No	8 (7.0)	36 (31.6)	
Presence or absence of washout when IW is allowed				
PP/PP	Yes	91 (79.8)	81 (71.1)	0.078
	No	23 (20.2)	33 (28.9)	
PP/DP	Yes	91 (79.8)	93 (81.6)	0.845
	No	23 (20.2)	21 (18.4)	
TP/DP	Yes	108 (94.7)	93 (81.6)	0.004
	No	6 (5.3)	21 (18.4)	

Data are number of lesions with percentages in parentheses. Washout was defined as negative visual SIR in each phase with temporal reduction of visual SIR from arterial phase to the phase. DP = delayed phase, ECA = extracellular agent, HBA = hepatobiliary agent, IW = illusional washout, PP = portal venous phase, SIR = signal intensity ratio, TP = transitional phase

(83.3% vs. 90.9%; p = 0.228), and the addition of IW did not increase the sensitivities on both MRIs.

The sensitivity of the modified LR-5 criteria using TP washout was higher than that of the LR-5 criteria using DP washout in all tumors (91.2% vs. 73.7%; p < 0.001) and in tumors smaller than 20 mm (89.6% vs. 50.0%; p < 0.001). When IW was also allowed, the differences were smaller in all tumors (91.2% vs. 82.5%; p = 0.055) and in tumors smaller than 20 mm (89.6% vs. 70.8%; p = 0.027).

DISCUSSION

In this intraindividual comparison study, the frequency of extracellular phase washout was comparable between MRIs with HBA and ECA. The LR-5 criteria using extracellular phase washout showed a comparable sensitivity for HCC on both MRIs (78.1% for HBA-MRI vs. 73.7% for ECA-MRI), except for tumors smaller than 20 mm. We also found that allowing IW, defined as an isointensity of the lesion to the liver in the presence of an enhancing capsule, as washout could improve sensitivity for the diagnosis of HCC on ECA-MRI, especially for tumors smaller than 20 mm (from 73.7% to 82.5% in all lesions, and from 50.0% to 70.8% in lesions smaller than 20 mm). Considering that it is not always feasible to strictly differentiate IW from true washout by visual assessment, regarding IW as washout may facilitate radiologist's decision and improve sensitivity for HCC diagnosis.

Interestingly, PP washout was more common with HBA-MRI than with ECA-MRI. PP is generally considered to begin approximately at 50–70 seconds and last up to 90 seconds after injection of gadoxetic acid [11,17-19], while liver parenchymal enhancement is observed as early as 60–90 seconds after contrast injection [13,14]. In our study, visual SIR in the PP was lower on HBA-MRI than on ECA-MRI, which is similar to the findings of other studies [20,21]. Therefore, liver parenchymal enhancement with HBA-MRI appears to start shortly after or even during PP [22]. Additionally, DP washout with ECA-MRI was more frequent than PP washout with ECA-MRI, as previously observed [17,23]. Although restricting the definition of washout to only PP may fail to encompass the varying washout patterns of HCC according to histological architectures [12], the frequency of PP washout with HBA-MRI can at least be comparable to that of DP washout with ECA-MRI owing to the appreciable liver parenchymal enhancement in PP. However, the possibility of a false-positive diagnosis of HCC with PP washout on HBA-MRI is unknown, which requires further study.

We discovered that extracellular phase washout was comparable between both MRIs, which was in concordance with a previous report [7]. Surprisingly, only half of the tumors smaller than 20 mm met the LR-5 criteria with ECA-MRI in this study. However, it should be noted that IW, a subjective optical illusion in the presence of an enhancing capsule [4], was strictly differentiated from washout by evaluating visual SIR in order to validate the LI-RADS washout definition. Among various guidelines for HCC diagnosis, only LI-RADS and Organ Procurement and Transplantation Network criteria employ an enhancing capsule as a major feature for the diagnosis of HCC [24]. The value of enhancing capsule in overall diagnostic performance has been deemed questionable since an enhancing capsule commonly appears together with washout in nodules 20 mm or smaller according to Rimola et al. [25]. Our analysis showed that allowing IW as washout, possibly done in prior studies, can increase the sensitivity for HCC diagnosis in tumors smaller than 20 mm. Although we did not measure the specificity for HCC diagnosis, it would not be significantly impaired by allowing IW since an enhancing capsule is a feature highly specific for HCC, and hepatocellular adenoma is the only non-HCC entity that may
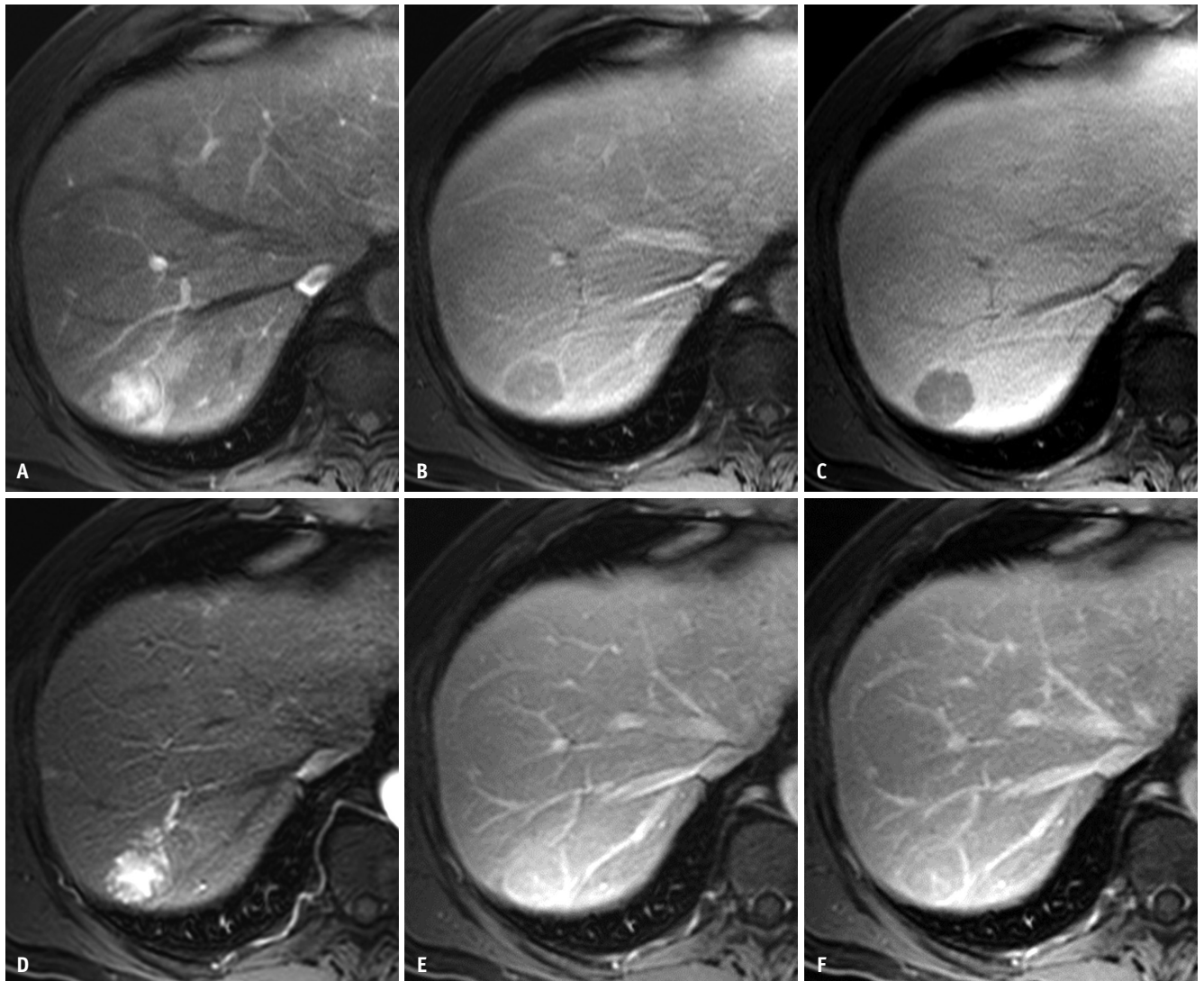
Fig. 3. A 60-year-old man with hepatitis B-related liver cirrhosis and hepatocellular carcinoma.
A-C. On the axial T1-weighted 3D turbo field-echo images obtained after gadoxetic acid injection, a 30-mm mass at hepatic segment VII shows **(A)** non-rim APHE (visual SIR, +2), **(B)** PP washout (visual SIR, -1; temporal reduction in enhancement from AP, -3) as well as an enhancing capsule, and **(C)** transitional phase washout (visual SIR, -2; a temporal reduction from AP, -4). **D-F.** On the axial T1-weighted 3D turbo field-echo images obtained after gadoterate meglumine administration, the mass reveals **(D)** non-rim APHE (visual SIR, +2). Isointensities in **(E)** PP (visual SIR, 0) and **(F)** delayed phase (visual SIR, 0) and an enhancing capsule indicate IW. LR-5 category was assigned on both MRIs by both readers. However, true washout is present only with hepatobiliary agent-enhanced MRI, while IW is observed with extracellular agent-enhanced MRI. AP = arterial phase, APHE = arterial phase hyperenhancement, IW = illusional washout, LR-5 = Liver Imaging Reporting and Data System category 5, PP = portal venous phase, SIR = signal intensity ratio, 3D = three-dimensional

exhibit non-rim APHE and an enhancing capsule [7,25,26]. Nevertheless, a 10–19 mm observation with non-rim APHE and an enhancing capsule is currently categorized as LR-4 in LI-RADS v2018. Future research is needed to validate the incremental value of IW in the overall diagnostic performance for HCCs smaller than 20 mm.

As expected, TP washout was more frequent than DP washout, and the sensitivity of the LR-5 criteria was higher using TP washout than that using DP washout, particularly in tumors smaller than 20 mm. However, it should be noted

that TP washout may only be allowed after exclusion of hemangiomas and non-HCC malignancies to maintain an acceptable specificity for HCC according to recent studies [27,28].

Our study has a few limitations. First, a selection bias may have been introduced by including only surgically resected HCCs. Nonetheless, a reference standard using the histopathology could have been the most accurate option as the possibility of non-HCC malignancy could be excluded. Second, we could not evaluate the specificity

measure for HCC diagnosis in our analysis. Nonetheless, we suppose that using IW in non-targetoid lesions will not significantly impair the specificity of LR-5 criteria since an enhancing capsule is highly specific for HCC [25], and the non-targetoid criteria, by definition, increase the specificity of LR-5 criteria [3]. Given that the LI-RADS criteria are
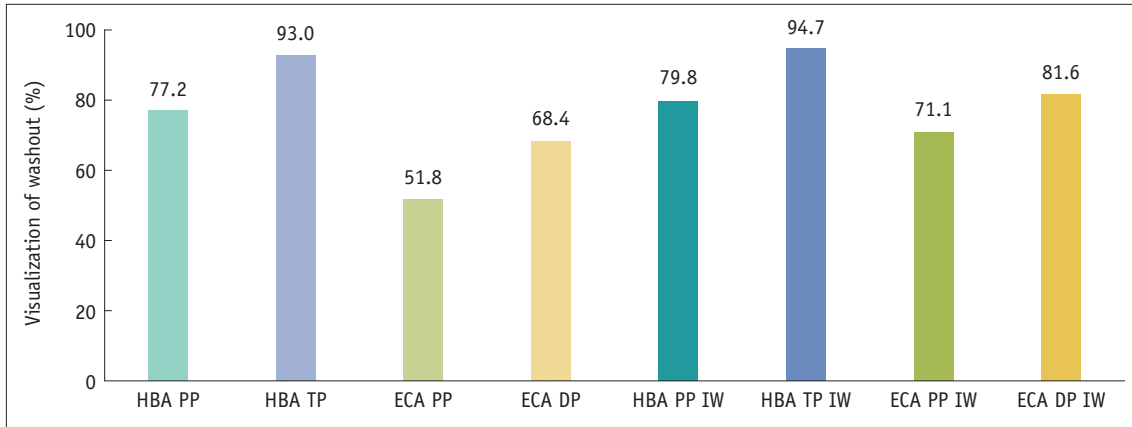

Fig. 4. Frequency of washout according to MRI contrast media. TP indicates washout assessed in TP. IW indicates incorporating IW in the washout definition. DP = delayed phase, ECA = extracellular agent, HBA = hepatobiliary agent, IW = illusional washout, PP = portal venous phase, TP = transitional phase

Table 4. Sensitivity for Hepatocellular Carcinoma according to Washout Definition

Phase (HBA/ECA)	HBA	ECA	P	HBA-IW*	ECA-IW*	P
All size (n = 114)						
PP/DP	89 (78.1)	84 (73.7)	0.458	90 (79.0)	94 (82.5)	0.540
TP[†]/DP	104 (91.2)	84 (73.7)	< 0.001	104 (91.2)	94 (82.5)	0.055
Size < 20 mm (n = 48)						
PP/DP	34 (70.8)	24 (50.0)	0.034	35 (72.9)	34 (70.8)	> 0.999
TP[†]/DP	43 (89.6)	24 (50.0)	< 0.001	43 (89.6)	34 (70.8)	0.027
Size ≥ 20 mm (n = 66)						
PP/DP	55 (83.3)	60 (90.9)	0.228	55 (83.3)	60 (90.9)	0.228
TP[†]/DP	61 (92.4)	60 (90.9)	> 0.999	61 (92.4)	60 (90.9)	> 0.999

Data are number of lesions satisfying the LR-5 or modified LR-5 criteria with the sensitivity measures in parentheses. *Modified LR-5 criteria allowing IW as washout, [†]Modified LR-5 criteria allowing TP washout as washout for HBA-MRI. DP = delayed phase, ECA = extracellular agent, HBA = hepatobiliary agent, IW = illusional washout, LR-5 = Liver Imaging Reporting and Data System category 5, PP = portal venous phase, TP = transitional phase
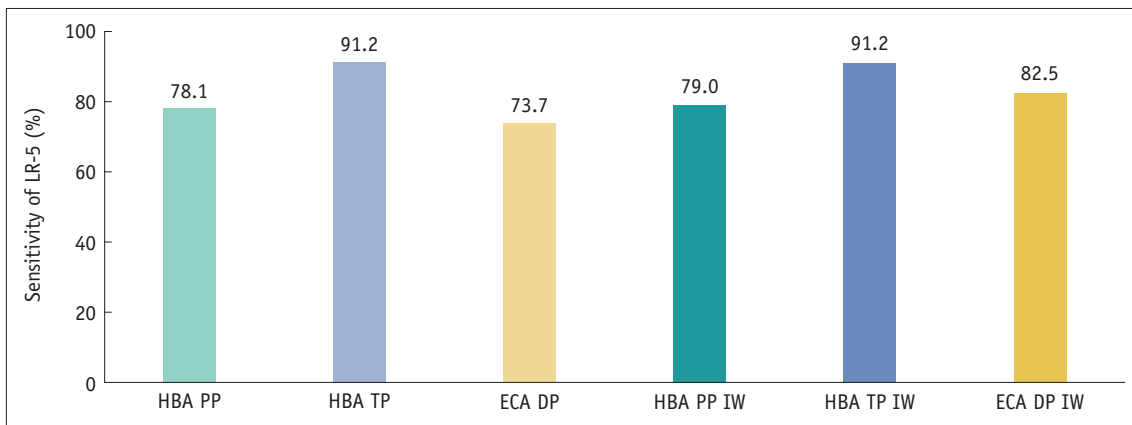
Fig. 5. Sensitivity of LR-5 criteria for hepatocellular carcinoma according to washout definition. As modified LR-5 criteria, TP indicates using washout assessed in TP, and IW indicates allowing IW as washout. DP = delayed phase, ECA = extracellular agent, HBA = hepatobiliary agent, IW = illusional washout, LR-5 = Liver Imaging Reporting and Data System category 5, PP = portal venous phase, TP = transitional phase

designed to achieve high specificity for the diagnosis of HCC, the question persists as how to allow for modifications in the current criteria to maintain high specificity. Future intraindividual comparison studies on LI-RADS, including a large number of non-HCC lesions, are warranted. Third, qualitative analysis using visual SIR may be difficult to reflect a subtle temporal reduction in enhancement. However, we did not perform a quantitative analysis as LI-RADS recommends the visual assessment of washout. Additionally, accurate measurement of noise is difficult when using parallel imaging [29]. Lastly, this is a single-center study with the majority of patients with hepatitis B virus infection and Child-Pugh class A, which might somewhat limit the generalizability of our study results.

In conclusion, the extracellular phase washout for HCC diagnosis may be comparable between MRIs with HBA and ECA, except for tumors smaller than 20 mm. Adding IW could improve the sensitivity for HCC on ECA-MRI in tumors smaller than 20 mm.

Conflicts of Interest

The authors have no potential conflicts of interest to disclose.

Author Contributions

Conceptualization: Young Kon Kim. Data curation: Yeun-Yoon Kim, Ji Hye Min, Dong Ik Cha, Jong Man Kim, Gyu-Seong Choi. Formal analysis: Yeun-Yoon Kim, Soohyun Ahn. Investigation: Yeun-Yoon Kim, Ji Hye Min, Dong Ik Cha. Methodology: Young Kon Kim, Yeun-Yoon Kim. Project administration: Young Kon Kim. Supervision: Young Kon Kim. Validation: Young Kon Kim. Visualization: Yeun-Yoon Kim. Writing—original draft: Yeun-Yoon Kim. Writing—review & editing: Young Kon Kim, Ji Hye Min, Dong Ik Cha, Jong Man Kim, Gyu-Seong Choi, Soohyun Ahn.

ORCID iDs

Yeun-Yoon Kim
  https://orcid.org/0000-0003-2018-5332
Young Kon Kim
  https://orcid.org/0000-0002-6854-400X
Ji Hye Min
  https://orcid.org/0000-0002-8496-6771
Dong Ik Cha
  https://orcid.org/0000-0003-3271-6532
Jong Man Kim
  https://orcid.org/0000-0002-1903-8354
Gyu-Seong Choi
  https://orcid.org/0000-0003-2545-3105
Soohyun Ahn
  https://orcid.org/0000-0001-5016-5469

REFERENCES

1. Kim TH, Kim SY, Tang A, Lee JM. Comparison of international guidelines for noninvasive diagnosis of hepatocellular carcinoma: 2018 update. *Clin Mol Hepatol* 2019;25:245-263
2. Tang A, Bashir MR, Corwin MT, Cruite I, Dietrich CF, Do RKG, et al. Evidence supporting LI-RADS major features for CT-and MR imaging–based diagnosis of hepatocellular carcinoma: a systematic review. *Radiology* 2018;286:29-48
3. Kim YY, Kim MJ, Kim EH, Roh YH, An C. Hepatocellular carcinoma versus other hepatic malignancy in cirrhosis: performance of LI-RADS version 2018. *Radiology* 2019;291:72-80
4. Sofue K, Sirlin CB, Allen BC, Nelson RC, Berg CL, Bashir MR. How reader perception of capsule affects interpretation of washout in hypervascular liver nodules in patients at risk for hepatocellular carcinoma. *J Magn Reson Imaging* 2016;43:1337-1345
5. Stocker D, Becker AS, Barth BK, Skawran S, Kaniewska M, Fischer MA, et al. Does quantitative assessment of arterial phase hyperenhancement and washout improve LI-RADS v2018-based classification of liver lesions? *Eur Radiol* 2020;30:2922-2933
6. Chernyak V, Fowler KJ, Kamaya A, Kielar AZ, Elsayes KM, Bashir MR, et al. Liver Imaging Reporting and Data System (LI-RADS) version 2018: imaging of hepatocellular carcinoma in at-risk patients. *Radiology* 2018;289:816-830
7. Min JH, Kim JM, Kim YK, Kang TW, Lee SJ, Choi GS, et al. Prospective intraindividual comparison of magnetic resonance imaging with gadoxetic acid and extracellular contrast for diagnosis of hepatocellular carcinomas using the Liver Imaging Reporting and Data System. *Hepatology* 2018;68:2254-2266
8. Hamm B, Staks T, Mühler A, Bollow M, Taupitz M, Frenzel T, et al. Phase I clinical evaluation of Gd-EOB-DTPA as a hepatobiliary MR contrast agent: safety, pharmacokinetics, and MR imaging. *Radiology* 1995;195:785-792
9. Doo KW, Lee CH, Choi JW, Lee J, Kim KA, Park CM. "Pseudo washout" sign in high-flow hepatic hemangioma on gadoxetic acid contrast-enhanced MRI mimicking hypervascular tumor. *AJR Am J Roentgenol* 2009;193:W490-W496
10. Joo I, Lee JM, Lee DH, Jeon JH, Han JK, Choi BI. Noninvasive diagnosis of hepatocellular carcinoma on gadoxetic acid-enhanced MRI: can hypointensity on the hepatobiliary phase be used as an alternative to washout? *Eur Radiol* 2015;25:2859-2868
11. Zech CJ, Ba-Ssalamah A, Berg T, Chandarana H, Chau GY, Grazioli L, et al. Consensus report from the 8th International

Forum for Liver Magnetic Resonance Imaging. *Eur Radiol* 2020;30:370-382

12. Okamoto D, Yoshimitsu K, Nishie A, Tajima T, Asayama Y, Ishigami K, et al. Enhancement pattern analysis of hypervascular hepatocellular carcinoma on dynamic MR imaging with histopathological correlation: validity of portal phase imaging for predicting tumor grade. *Eur J Radiol* 2012;81:1116-1121

13. Vogl TJ, Kümmel S, Hammerstingl R, Schellenbeck M, Schumacher G, Balzer T, et al. Liver tumors: comparison of MR imaging with Gd-EOB-DTPA and Gd-DTPA. *Radiology* 1996;200:59-67

14. Reimer P, Rummeny EJ, Daldrup HE, Hesse T, Balzer T, Tombach B, et al. Enhancement characteristics of liver metastases, hepatocellular carcinomas, and hemangiomas with Gd-EOB-DTPA: preliminary results with dynamic MR imaging. *Eur Radiol* 1997;7:275-280

15. Lebert P, Adens-Fauquembergue M, Azahaf M, Gnemmi V, Behal H, Luciani A, et al. MRI for characterization of benign hepatocellular tumors on hepatobiliary phase: the added value of in-phase imaging and lesion-to-liver visual signal intensity ratio. *Eur Radiol* 2019;29:5742-5751

16. Santillan C, Fowler K, Kono Y, Chernyak V. LI-RADS major features: CT, MRI with extracellular agents, and MRI with hepatobiliary agents. *Abdom Radiol (NY)* 2018;43:75-81

17. Allen BC, Ho LM, Jaffe TA, Miller CM, Mazurowski MA, Bashir MR. Comparison of visualization rates of LI-RADS version 2014 major features with IV gadobenate dimeglumine or gadoxetate disodium in patients at risk for hepatocellular carcinoma. *AJR Am J Roentgenol* 2018;210:1266-1272

18. Agnello F, Dioguardi Burgio M, Picone D, Vernuccio F, Cabibbo G, Giannitrapani L, et al. Magnetic resonance imaging of the cirrhotic liver in the era of gadoxetic acid. *World J Gastroenterol* 2016;22:103-111

19. Tamada T, Ito K, Yamamoto A, Yasokawa K, Higaki A, Kanki A, et al. Simple method for evaluating the degree of liver parenchymal enhancement in the hepatobiliary phase of gadoxetic acid-enhanced magnetic resonance imaging. *J Magn Reson Imaging* 2013;37:1115-1121

20. Kim YN, Song JS, Moon WS, Hwang HP, Kim YK. Intra-individual comparison of hepatocellular carcinoma imaging features on contrast-enhanced computed tomography, gadopentetate dimeglumine-enhanced MRI, and gadoxetic acid-enhanced MRI. *Acta Radiol* 2018;59:639-648

21. Son J, Hwang SH, Park S, Han K, Chung YE, Choi JY, et al. Imaging features of hepatocellular carcinoma: quantitative and qualitative comparison between MRI-enhanced with Gd-EOB-DTPA and Gd-DTPA. *Invest Radiol* 2019;54:494-499

22. Goodwin MD, Dobson JE, Sirlin CB, Lim BG, Stella DL. Diagnostic challenges and pitfalls in MR imaging with hepatocyte-specific contrast agents. *Radiographics* 2011;31:1547-1568

23. Cereser L, Furlan A, Bagatto D, Girometti R, Como G, Avellini C, et al. Comparison of portal venous and delayed phases of gadolinium-enhanced magnetic resonance imaging study of cirrhotic liver for the detection of contrast washout of hypervascular hepatocellular carcinoma. *J Comput Assist Tomogr* 2010;34:706-711

24. Wald C, Russo MW, Heimbach JK, Hussain HK, Pomfret EA, Bruix J. New OPTN/UNOS policy for liver transplant allocation: standardization of liver imaging, diagnosis, classification, and reporting of hepatocellular carcinoma. *Radiology* 2013;266:376-382

25. Rimola J, Forner A, Tremosini S, Reig M, Vilana R, Bianchi L, et al. Non-invasive diagnosis of hepatocellular carcinoma ≤ 2 cm in cirrhosis. Diagnostic accuracy assessing fat, capsule and signal intensity at dynamic MRI. *J Hepatol* 2012;56:1317-1323

26. Grazioli L, Olivetti L, Mazza G, Bondioni MP. MR imaging of hepatocellular adenomas and differential diagnosis dilemma. *Int J Hepatol* 2013;2013:374170

27. Joo I, Lee JM, Lee DH, Jeon JH, Han JK. Retrospective validation of a new diagnostic criterion for hepatocellular carcinoma on gadoxetic acid-enhanced MRI: can hypointensity on the hepatobiliary phase be used as an alternative to washout with the aid of ancillary features? *Eur Radiol* 2019;29:1724-1732

28. Kim DH, Choi SH, Kim SY, Kim MJ, Lee SS, Byun JH. Gadoxetic acid–enhanced MRI of hepatocellular carcinoma: value of washout in transitional and hepatobiliary phases. *Radiology* 2019;291:651-657

29. Heverhagen JT. Noise measurement and estimation in MR imaging experiments. *Radiology* 2007;245:638-639